

Observational constraints on higher-order gravity theory

Harshna Balhara
PhD Research Scholar

Netaji Subhas University of Technology
Delhi, India

September, 2023

Collaborators
Prof. J K Singh, Prof. Kazuharu Bamba, Shaily



Outline

- 1 Einstein field equations for $\mathcal{F}(\mathcal{R}, \mathcal{G})$ gravity
- 2 Observational Constraints
- 3 Physical behavior of Cosmological Parameters
- 4 Energy Conditions
- 5 Statefinder Diagnostics
- 6 Conclusion
- 7 References



Outline

- 1 Einstein field equations for $\mathcal{F}(\mathcal{R}, \mathcal{G})$ gravity
- 2 Observational Constraints
- 3 Physical behavior of Cosmological Parameters
- 4 Energy Conditions
- 5 Statefinder Diagnostics
- 6 Conclusion
- 7 References



Solution

- The gravitational action of $\mathcal{F}(\mathcal{R}, \mathcal{G})$ gravity is [1, 2]

$$\mathcal{S} = \frac{1}{2\kappa} \int \mathcal{F}(\mathcal{R}, \mathcal{G}) \sqrt{-g} d^4x + \int \mathcal{L}_m \sqrt{-g} d^4x, \quad (1)$$

where \mathcal{R} is the Ricci scalar, g is the determinant of the metric tensor $g_{\mu\nu}$ and \mathcal{G} is the Gauss-Bonnet invariant defined as

$$\mathcal{G} = \mathcal{R}^2 - 4\mathcal{R}_{ij}\mathcal{R}^{ij} + \mathcal{R}_{ijkl}\mathcal{R}^{ijkl}, \quad (2)$$

\mathcal{L}_m is the matter Lagrangian density, \mathcal{R}_{ij} is the Ricci tensor, \mathcal{R}_{ijkl} is the Riemann tensor and $\kappa = 8\pi G$.



- The Hubble parameter $H = \dot{a}(t)/a(t)$, which measures the expansion rate of the universe, may be used to describe the Ricci scalar \mathcal{R} and Gauss-Bonnet term \mathcal{G} as

$$\mathcal{R} = 6(\dot{H} + 2H^2), \quad \mathcal{G} = 24H^2(\dot{H} + H^2)$$

respectively, here dot represents derivative with respect to the cosmic time t .

- The energy-momentum tensor for perfect fluid is given as

$$T_{ij} = (\rho + p)u_i u_j + p g_{ij},$$

where ρ and p stand for the matter-energy density and matter pressure respectively.

- The cosmic fluid's time-like four-velocity vector u^i satisfies the property $u_i u^i = 1$



- The gravitational field equations for a flat Friedmann-Lemaitre-Robertson-Walker (FLRW) space-time

$$ds^2 = -dt^2 + a^2(t)(dx^2 + dy^2 + dz^2), \quad (3)$$

can be given, see Cognola et al. [3] as

$$3H^2 = \frac{\kappa^2}{\mathcal{F}_{\mathcal{R}}} \rho + \frac{1}{2} \left[\mathcal{R} + \mathcal{G} \frac{\mathcal{F}_{\mathcal{G}}}{\mathcal{F}_{\mathcal{R}}} - \frac{\mathcal{F}(\mathcal{R}, \mathcal{G})}{\mathcal{F}_{\mathcal{R}}} \right] - 3H \frac{\dot{\mathcal{F}}_{\mathcal{R}}}{\mathcal{F}_{\mathcal{R}}} - 12H^3 \frac{\dot{\mathcal{F}}_{\mathcal{G}}}{\mathcal{F}_{\mathcal{R}}} \quad (4)$$

$$2\dot{H} + 3H^2 = \frac{-\kappa^2}{\mathcal{F}_{\mathcal{R}}} p + \frac{1}{2} \left[\mathcal{F}_{\mathcal{R}} + \mathcal{G} \frac{\mathcal{F}_{\mathcal{G}}}{\mathcal{F}_{\mathcal{R}}} - \frac{\mathcal{F}(\mathcal{R}, \mathcal{G})}{\mathcal{F}_{\mathcal{R}}} \right] - 2H \frac{\dot{\mathcal{F}}_{\mathcal{R}}}{\mathcal{F}_{\mathcal{R}}} - \frac{\ddot{\mathcal{F}}_{\mathcal{R}}}{\mathcal{F}_{\mathcal{R}}} - 4H^2 \frac{\ddot{\mathcal{F}}_{\mathcal{G}}}{\mathcal{F}_{\mathcal{R}}} - 8H(\dot{H} + H^2) \frac{\dot{\mathcal{F}}_{\mathcal{G}}}{\mathcal{F}_{\mathcal{R}}} \quad (5)$$



- The function $\mathcal{F}(\mathcal{R}, \mathcal{G})$ is assumed in explicit form as [1, 4]:

$$\mathcal{F}(\mathcal{R}, \mathcal{G}) = \mathcal{R} + \gamma\mathcal{G}^2, \quad (6)$$

where γ is an arbitrary constant.

- By using the specific form of $\mathcal{F}(\mathcal{R}, \mathcal{G})$ given by Eq. (6), Eqs. (4) and (5) take the form:

$$\rho = \frac{1}{\kappa^2} \left(3H^2 - 288\gamma(\dot{H}^2 H^4 + H^8 + 2H^6 \dot{H}) + 576\gamma(2H^4 \dot{H} + H^2 \ddot{H} + 4H^3 \dot{H}) \right) \quad (7)$$

$$\begin{aligned} p = & 288\gamma(\dot{H}^2 H^4 + H^8 + 2H^6 \dot{H}) - 2\dot{H} - 3H^2 \\ & - 192\gamma H^2 \left(2\dot{H}^3 + 6H\dot{H}\ddot{H} + H^2 \ddot{H} + 12H^2 \dot{H}^2 + 4H^3 \ddot{H} \right) \\ & - 348\gamma(H^3 + \dot{H}H)(2H\dot{H}^2 + H^2 \ddot{H} + 4H^3 \dot{H}) \quad (8) \end{aligned}$$



- It can be observed that the pressure p and energy density ρ are dependent on the Hubble parameter H and its time derivatives. In the current scenario, an additional constraint equation is needed to fully solve the system of field equations.
- We impose a constraint on the Hubble parameter. The motivation behind choosing the parametric form of the Hubble parameter H is to discuss the dark energy model together with the transition from deceleration to acceleration at present as well as in the future, which has been discussed in some recent works [5, 6, 7].

$$H = \alpha(\beta + a^{-n}), \quad (9)$$

where $\alpha, \beta > 0, n > 1$ are model parameters and a is scale factor.

- Eq. (9) yields

$$a(t) = \left(-\frac{1 - e^{\alpha\beta nt + \beta c_1 n}}{\beta} \right)^{1/n}, \quad (10)$$

where c_1 is an arbitrary constant of integration which may be taken as zero.



- The scale factor a in terms of redshift z is defined as $\frac{a_0}{a} = 1 + z$, with normalized scale factor $a_0 = 1$, Eq. (10) yields

$$t(z) = \frac{\log \left(1 + \beta \left(\frac{1}{z+1} \right)^n \right)}{\alpha \beta n}. \quad (11)$$

- The Hubble parameter H in terms of the redshift z , which explains the dynamics of the universe can be expressed as

$$H(z) = \alpha \left(\beta - \frac{\beta}{\beta \left(-\frac{1}{\beta} - \left(\frac{1}{z+1} \right)^n \right) + 1} \right). \quad (12)$$



Outline

- 1 Einstein field equations for $\mathcal{F}(\mathcal{R}, \mathcal{G})$ gravity
- 2 Observational Constraints**
- 3 Physical behavior of Cosmological Parameters
- 4 Energy Conditions
- 5 Statefinder Diagnostics
- 6 Conclusion
- 7 References



Observational Constraints

- The model parameters α , β , and n have been constrained by employing the MCMC sampling technique with the Python emcee [8] library.
- We find the best-fit values of the model parameters to validate our model using the current observational Pantheon dataset of 1048 points from the low redshift range $z \in (0.01, 2.26)$ [10, 11] and Hubble H_z dataset of 77 points [12, 13, 14].



Hubble Dataset

- The Hubble parameter in terms of redshift z can be expressed as $H(z) = -\frac{1}{z} \frac{dz}{dt}$, where $\frac{dz}{dt}$ is determined from spectroscopic surveys.
- In our analysis, we have employed a standard compilation of 77 measures from Hubble data [14]. Also, we have used $H_0 = 69 \text{Km/s/Mpc}$ for our analysis.
- The minimum chi-square function (χ_{min}^2) obtained by the maximum likelihood analysis, which is used to determine the average values of the model parameters is given by

$$\chi_{Hub}^2 = \sum_i^{77} \frac{[H_{th}(z_i, \mathcal{P}) - H_{obs}(z_i)]^2}{\sigma_{(z_i)}^2}, \quad (13)$$

Here, $H_{th}(z_i, \mathcal{P})$ is the theoretical value for the given model at redshift z_i , and \mathcal{P} denotes the parameter space. The observational value is denoted by $H_{obs}(z_i)$, and the error is denoted by $\sigma_{(z_i)}^2$.



Hubble Dataset

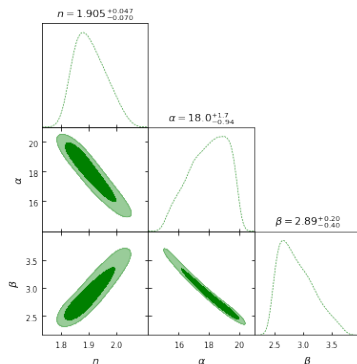


Figure 1: The $1 - \sigma$ and $2 - \sigma$ likelihood contours for the best-fit values of the model parameters using the $H(z)$ dataset.

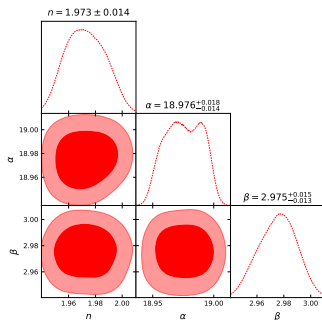


Pantheon Dataset

The χ_{Pan}^2 function is needed for the Pantheon datasets in the form of,

$$\chi_{Pan}^2 = \sum_{i=1}^{1048} \left[\frac{\mu_{th}(H_0, \mathcal{P}) - \mu_{obs}(z_i)}{\sigma_{\mu(z_i)}} \right]^2, \quad (14)$$

where the standard error of the observed value is denoted by $\sigma_{\mu(z_i)}$.



H_z+Pantheon Dataset

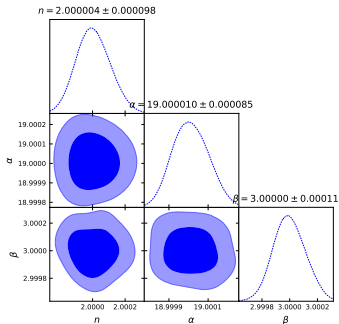


Figure 2: The $1 - \sigma$ and $2 - \sigma$ likelihood contours for the best-fit values of the model parameters using the Joint dataset.



Error Bar Plot

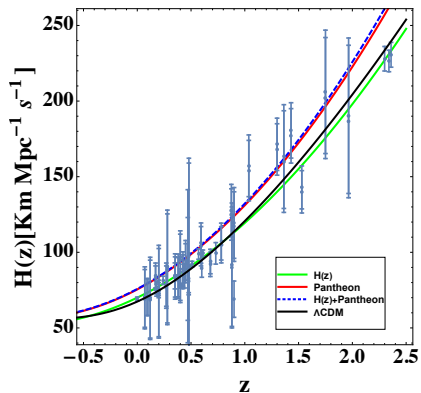


Figure 3: Error bar plot using 77 points of Hubble data vs redshift z compared to ΛCDM model.



Outline

- 1 Einstein field equations for $\mathcal{F}(\mathcal{R}, \mathcal{G})$ gravity
- 2 Observational Constraints
- 3 Physical behavior of Cosmological Parameters**
- 4 Energy Conditions
- 5 Statefinder Diagnostics
- 6 Conclusion
- 7 References



Deceleration Parameter

- The rate of acceleration of the universe is described by deceleration parameter q .
- It is a function of the Hubble parameter and has the form $q = -1 - \frac{\dot{H}}{H^2}$.
- If $q > 0$: This implies that the universe's expansion is slowing down over time due to gravitational attraction. In this case, the universe is said to be in a decelerating phase.
- If $q < 0$: This suggests that the universe's expansion is accelerating over time. This acceleration could be due to the presence of a form of energy with negative pressure, like dark energy. A universe with negative q is said to be in an accelerating phase.



- Using the value of H and substituting in $q = -1 - \frac{\dot{H}}{H^2}$ gives

$$q(z) = -\frac{\beta^3 n \left(-\frac{1}{\beta} - \left(\frac{1}{z+1} \right)^n \right)}{\left(\beta \left(-\frac{1}{\beta} - \left(\frac{1}{z+1} \right)^n \right) + 1 \right)^2 \left(\beta - \frac{\beta}{\beta \left(-\frac{1}{\beta} - \left(\frac{1}{z+1} \right)^n \right) + 1} \right)^2} - 1, \quad (15)$$

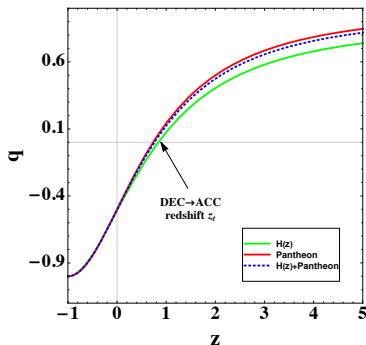


Figure 4: The evolution of the deceleration parameter q for the constraint values of the model parameters obtained from various observational datasets.



Equation of State Parameter (ω)

- Mathematically, the equation of state parameter is defined as:

$$\omega = \frac{p}{\rho}$$

where p is the pressure and ρ the energy density.

- $-1 < \omega < 0$ (Quintessence phase): If the equation of state parameter is greater than -1, it indicates that the substance has positive pressure relative to its energy density. This corresponds to a repulsive force that accelerates the universe's expansion.
- $\omega < -1$ (Phantom Phase): This scenario can lead to a more rapid expansion of the universe, potentially leading to a "Big Rip" scenario where the expansion becomes unbounded.
- $\omega = 0$ (Dust Phase): If the equation of state parameter is 0, it implies that the substance's pressure is negligible compared to its energy density.
- $\omega = 1/3$, (radiation-dominated phase): Radiation has a positive pressure $p = \frac{1}{3}\rho$ and contributes differently to the expansion of the universe compared to non-relativistic matter.



Evolution of EoS Parameter, Energy Density and pressure

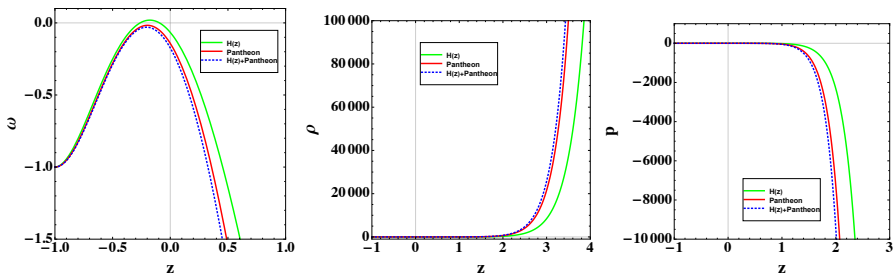


Figure 5: Evolution of the EoS parameter ω , energy density ρ , and the pressure p for the constraint values of the model parameters obtained from various observational datasets.



Outline

- 1 Einstein field equations for $\mathcal{F}(\mathcal{R}, \mathcal{G})$ gravity
- 2 Observational Constraints
- 3 Physical behavior of Cosmological Parameters
- 4 Energy Conditions**
- 5 Statefinder Diagnostics
- 6 Conclusion
- 7 References



Energy Conditions

- The EC can be expressed in a variety of ways, including geometrically (in terms of the Ricci or Weyl tensors), physically (with the help of the stress energy-momentum tensor), or effectively (in terms of energy density, which serves as the time-like component, and pressure $p_i, i = 1, 2, 3$ which represent the 3-space-like component).
- In GR, the formulation of these four forms of EC is effectively represented as [17]:
- Null Energy Condition $\iff \rho + p_i \geq 0, \forall i$
- Weak Energy Condition $\iff \rho \geq 0, \rho + p_i \geq 0, \forall i$
- Strong Energy Condition $\iff \rho + \sum_{i=1}^3 p_i \geq 0, \rho + p_i \geq 0, \forall i;$
- Dominant Energy Condition $\iff \rho \geq 0, |p_i| \leq \rho, \forall i.$



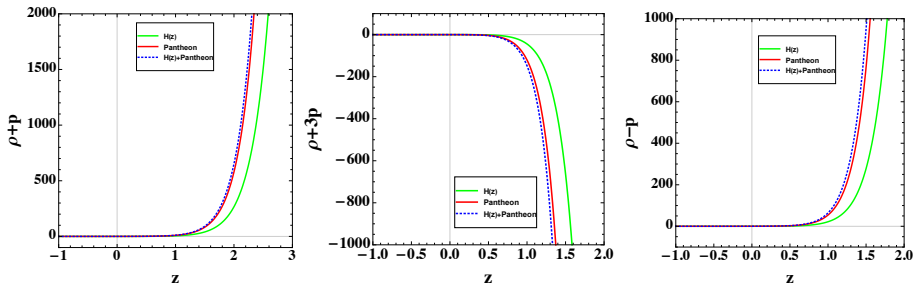


Figure 6: The graphical behavior of NEC, SEC, and DEC for the constraint values of the model parameters obtained from various observational datasets.



Outline

- 1 Einstein field equations for $\mathcal{F}(\mathcal{R}, \mathcal{G})$ gravity
- 2 Observational Constraints
- 3 Physical behavior of Cosmological Parameters
- 4 Energy Conditions
- 5 Statefinder Diagnostics**
- 6 Conclusion
- 7 References



Statefinder Diagnostics

- To distinguish all sorts of cosmological models Sahni et al. [18, 19] suggested utilizing a statefinder pair $\{r, s\}$.
- The parameters $\{r, s\}$ are defined as

$$r = \frac{\ddot{a}}{aH^3} = q(1 + 2q), \quad s = \frac{r - 1}{3\left(q - \frac{1}{2}\right)}, \quad (16)$$

where $q \neq 1/2$.

- In $s - r$ plane the statefinder coordinates $\{1, 0\}$, $\{1, 1\}$, and $\{1, \frac{2}{3}\}$ represent Λ CDM, $SCDM$, and HDE respectively.
- In $q - r$ plane, $\{1, -1\}$ represent the Steady state model while $\{\frac{1}{2}, 1\}$ represent the Standard Cold Dark Matter.



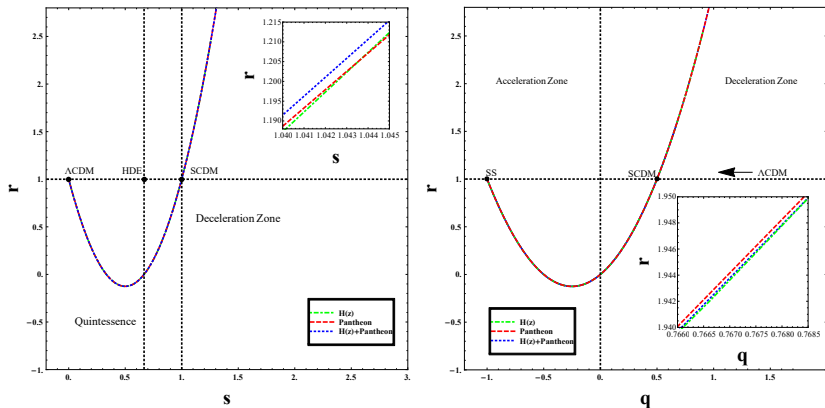


Figure 7: The behavior of $s - r$ and $q - r$ trajectories for the constraint values of the model parameters obtained from various observational datasets.

Outline

- 1 Einstein field equations for $\mathcal{F}(\mathcal{R}, \mathcal{G})$ gravity
- 2 Observational Constraints
- 3 Physical behavior of Cosmological Parameters
- 4 Energy Conditions
- 5 Statefinder Diagnostics
- 6 Conclusion**
- 7 References



Conclusion

- The likelihood contours with the best-fit values of the model parameters obtained by applying *emcee* codes in Python using the Hubble, pantheon, and joint dataset with $1 - \sigma$, $2 - \sigma$ confidence levels have been discussed.
- In Fig. 3, the error bar plot of $H(z)$ with respect to the redshift z depict that our model is consistent with Λ CDM for all the observational dataset $H(z)$ of 77-points, *Pantheon* of 1048 points and the joint $H(z) + \textit{Pantheon}$, at the present epoch and in the future epoch.
- In our model, we observe that the deceleration parameter q transits from a decelerating state to an accelerating state, and the transition nodes vary in the range of redshift $0.731 \leq z_t \leq 0.856$.
- Eos parameter passes through the various stages of evolution of the universe as it shows the phantom model at the initial stage and the quintessence dark energy model in the late times.



- The energy conditions NEC and DEC are satisfied, while SEC is violated in the low redshift range which is related to the universe accelerating due to the presence of some dark energy (see Fig. 6).
- The Statefinder trajectories in the $s - r$ plane depicts the trajectories evolving from the vicinity of $SCDM$, entering into the quintessence region, and converging to Λ CDM. In the $q - r$ plane, the trajectories evolve from the decelerated zone, entering into the accelerated zone, and finally, converge to the SS model (see Fig. 7).











Outline

- 1 Einstein field equations for $\mathcal{F}(\mathcal{R}, \mathcal{G})$ gravity
- 2 Observational Constraints
- 3 Physical behavior of Cosmological Parameters
- 4 Energy Conditions
- 5 Statefinder Diagnostics
- 6 Conclusion
- 7 References**












References I

-  S. D. Odintsov, V. K. Oikonomou and S. Banerjee, Nucl. Phys. B **938**, 935-956 (2019).
-  N. Montelongo Garcia, F. S. N. Lobo, J. P. Mimoso and T. Harko, J. Phys. Conf. Ser. **314**, 012056 (2011).
-  G. Cognola, E. Elizalde, S. Nojiri, S. D. Odintsov and S. Zerbini, Phys. Rev. D **73** (2006), 084007
-  A. Kumar Sanyal and C. Sarkar, Class. Quant. Grav. **37**, no.5, 055010 (2020)
-  J. P. Singh, Astrophys. Space Sci. **318**, 103-107 (2008).
-  N. Banerjee and S. Das, Gen. Rel. Grav. **37**, 1695-1703 (2005).
-  R. Nagpal, S. K. J. Pacif, J. K. Singh, K. Bamba and A. Beesham, Eur. Phys. J. C **78**, no.11, 946, (2018).
-  D. Foreman-Mackey, D. W. Hogg, D. Lang and J. Goodman, Publ. Astron. Soc. Pac. **125**, 306-312 (2013).










References II

-  Y. L. Bolotin, V. A. Cherkaskiy, O. A. Lemets, D. A. Yerokhin and L. G. Zazunov,
-  D. M. Scolnic *et al.* [Pan-STARRS1], *Astrophys. J.* **859**, no.2, 101 (2018).
-  N. Suzuki *et al.* [Supernova Cosmology Project], *Astrophys. J.* **746**, 85, (2012).
-  H. Yu, B. Ratra and F. Y. Wang, *Astrophys. J.* **856**, no.1, 3 (2018).
-  M. Moresco, *Mon. Not. Roy. Astron. Soc.* **450**, no.1, L16-L20 (2015).
-  Shaily, M. Zeyauddin and J. K. Singh, [arXiv:2207.05076 [gr-qc]].
-  O. Farooq and B. Ratra, *Astrophys. J. Lett.* **766**, L7 (2013)
-  S. Capozziello, O. Farooq, O. Luongo and B. Ratra, *Phys. Rev. D* **90**, no.4, 044016 (2014)
-  E. A. Kontou and K. Sanders, *Class. Quant. Grav.* **37** (2020) no.19, 193001.



References III

-  V. Sahni, T. D. Saini, A. A. Starobinsky and U. Alam, JETP Lett. **77**, 201-206 (2003).
-  U. Alam, V. Sahni, T. D. Saini and A. A. Starobinsky, Mon. Not. Roy. Astron. Soc. **344**, 1057 (2003).
-  T. P. Sotiriou and V. Faraoni, Rev. Mod. Phys. **82**, 451-497 (2010).
-  A. De Felice and S. Tsujikawa, Living Rev. Rel. **13**, 3 (2010).
-  S. Nojiri and S. D. Odintsov, Phys. Rept. **505**, 59-144 (2011).
-  J. K. Singh, K. Bamba, R. Nagpal and S. K. J. Pacif, Phys. Rev. D **97**, no.12, 123536 (2018).
-  J. D. Barrow and S. Cotsakis, Phys. Lett. B **214**, 515-518 (1988).

